Citation for published version

Yan, Yong and Cui, Xiwang and Guo, Miao and Han, Xiaojuan (2016) Localization of a continuous CO2 leak from an isotropic flat-surface structure using acoustic emission detection and near-field beamforming techniques. Measurement Science and Technology, 27 (11). ISSN 0957-0233.

DOI

https://doi.org/10.1088/0957-0233/27/11/115105

Link to record in KAR

Document Version

Author's Accepted Manuscript

Localization of a continuous CO_2 leak from an isotropic flat-surface structure using acoustic emission detection and near-field beamforming techniques

Yong Yan[a,b], Xiwang Cui[a], Miao Guo[a] and Xiaojuan Han[a]
[a]*School of Control and Computer Engineering, North China Electric Power University, Beijing 102206, P R China*
[b]*School of Engineering and Digital Arts, University of Kent, Canterbury, Kent, CT2 7NT, UK*

Abstract

Seal capacity is of great importance for the safety operation of pressurized vessels. It is crucial to locate the leak hole timely and accurately for reasons of safety and maintenance. This paper presents the principle and application of a linear acoustic emission sensor array and a near-field beamforming technique to identify the location of a continuous CO_2 leak from an isotropic flat-surface structure on a pressurized vessel in the Carbon Capture and Storage system. Acoustic signals generated by the leak hole are collected using a linear high-frequency sensor array. Time-frequency analysis and a narrow-band filtering technique are deployed to extract effective information about the leak. The impacts of various factors on the performance of the localization technique are simulated, compared and discussed, including the number of sensors, distance between the leak hole and sensor array and spacing between adjacent sensors. Experiments were carried out on a laboratory-scale test rig to assess the effectiveness and operability of the proposed method. The results obtained suggest that the proposed method is capable of providing accurate and reliable localization of a continuous CO_2 leak.

Key words: CO_2 leak; Leak localization; Acoustic emission; Sensor array; Near-field beamforming

1. Introduction

Carbon Capture and Storage (CCS) is an emerging technology to reduce CO_2 emissions into the atmosphere from power generation and other industrial processes [1]. Pressurized vessels and containers are widely used in the process of CO_2 transportation. CO_2 leaks in these structures will influence the stability and safety of the CCS system and cause serious environmental pollution and economic losses. Therefore, it is crucial to locate the leak hole timely and accurately when it occurs. The practical storage vessel used in the CO_2 transportation process is commonly a spherical or cylindrical tank made of homogeneous and isotropic metal which is similar to the storage vessel used in the LNG (liquefied natural gas) transportation, so it is in fact a three-dimensional structure. Although the shell of the vessel is very large, if taking a small area of the shell to analyze and study in terms of leakage, we can treat this small area an isotropic flat-surface structure.

There are many kinds of gas leak detection and localization techniques like tracer gas, electromagnetic scanning, optical fiber sensing, infrared thermography and flow equilibrium [2-4]. Compared to other techniques, leak localization with acoustic emission (AE) technique has advantages of simple structure, low cost, non-intrusiveness, high sensitivity and easy installation and thus has a good potential for gas leak detection and localization [5].

A CO_2 leak from a pressurized vessel usually contains two stages. In the first stage, the metal shell of the pressurized vessel suddenly ruptures and then a leak hole emerges. In the second stage, the gas in the vessel flows through the leak hole to outside continuously. AE signals are generated in these two stages, which contain information about the leak hole such as location and size of the hole. The AE signal generated in the first stage is called burst-type signal and the AE signal generated in the second stage is called continuous-type signal, as shown in figure 1. Leak signals can be collected using AE sensors installed on the shell of the pressurized vessel. The localization of the leak hole is achieved using localization algorithms.

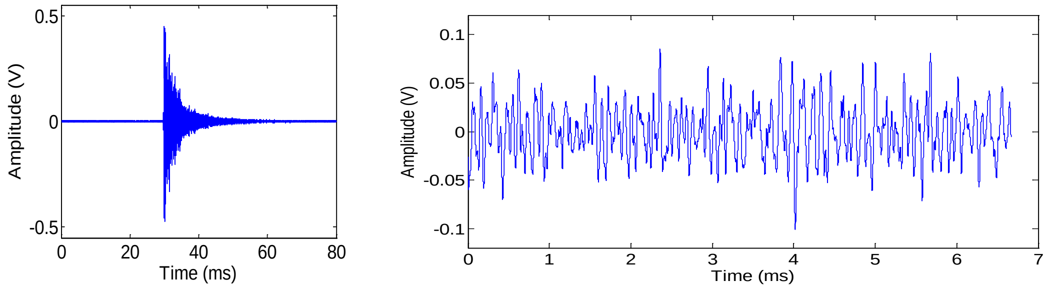

(a) Burst-type signal (b) Continuous-type signal

Figure 1. Typical leak signals

For the burst-type AE signal, the most common localization algorithm is the time difference of arrival (TDOA) [6] as it is easy to determine the time difference between different sensors because of the sharp rising edges in the time-domain waveforms, as shown in figure 1(a). The TDOA of different sensors can be measured through threshold-based procedures, peak detection techniques, and more robustly, cross correlation method [7, 8]. In order to locate the leak hole on a flat-surface structure, at least three sensors are required through the traditional triangulation method. There has been extensive research on the localization of the burst-type signal [9]. For the continuous AE signal, however, leak localization becomes more difficult and the traditional methods based on threshold and peak detection principles are ineffective because the first wave front is hard to identify in the time domain waveform (Figure 1(b)). Although the localization method based on cross-correlation analysis is feasible in theory, its accuracy and applicability are limited due to the signal attenuation and dispersion in the propagation along the shell of the pressurized vessel [10]. Therefore, more advanced signal filtering and decomposition techniques should be explored to improve the localization performance. Davoodi et al. proposed a method based on wavelet transform, filtering and cross-correlation techniques to locate a continuous leak source in underground high-pressure gas pipes [11]. Cui et al. investigated an empirical mode decomposition (EMD) and cross correlation method to improve the accuracy of localization [12]. Holland et al. developed an ultrasonic array sensor and a spatio-temporal Fourier transform technique based f-k analysis of cross correlations to find the leak direction in a manned spacecraft [13-15]. It is worth noting that two or more peak points with similar amplitude may appear and lead to a large localization error when calculating TDOA using the cross-correlation technique in some cases. In order to improve the localization performance, more practically feasible methods need to be developed.

Beamforming technique is an array signal processing method which identifies the signal source through scanning the whole area in question and identifying the peak point in the energy distribution graph. The beamforming technique is widely used in communication, radar, sonar and has achieved some successes [16]. However, this technique has rarely been applied for leak localization of gases in industry. In comparison with the TDOA approach, the beamforming method does not need to calculate the time difference between the leak signals, eliminating the requirement of complex signal processing before calculating the time difference. McLaskey et al. firstly used AE beamforming method in the damage localization of large structures in civil engineering [17]. He et al. used the beamforming method and AE sensors to diagnose the rub fault in rotating machinery. The experimental results demonstrated that the beamforming method could effectively determine the rubbing region [18]. Bian et al. proposed a far-field wideband beamforming localization method with an L-shaped sensor array to measure the angle of leak hole on a plate structure [19]. However, the far-field beamforming method requires very small AE sensors, a short distance between adjacent sensors and a long distance between the leak hole and the sensor array. These requirements may not be met in some practical cases, so a near-field model should be considered. To date there has been very little reported research on near-field beamforming methods for the localization of leaks from pressurized vessels, especially for continuous gaseous leaks. This paper proposed for the first time a near-field beamforming method combined with a linear AE sensor array for the localization of a continuous CO_2 leaks from an isotropic flat-surface structure. Numerical simulation and experimental studies are conducted to assess the localization accuracy, stability and influence factors.

2. Principle of Beamforming Technique

Localization methods based on the beamforming technique can be divided into the far-field model and the near-field model, depending on the distance between the leak hole and the sensor array. According to the empirical formula by Mailloux [20], the model can be regarded as near-field when equation 1 is satisfied, while the model will be considered as far-field if equation 2 is satisfied:

$$r \leq \frac{2L^2}{\lambda} \tag{1}$$

$$r > \frac{2L^2}{\lambda} \tag{2}$$

where *r* is the distance between the leak hole and the sensor array, *L* is the length of the linear array, and λ is the wavelength of the leak signal at a particular frequency. In the far-field model, the wave front curvature of the signal can be ignored and the acoustic wave can be regarded as a plane wave. In the near-field model, however, the wave front curvature cannot be ignored and the acoustic wave should be analyzed as a spherical wave, as shown in figure 2.

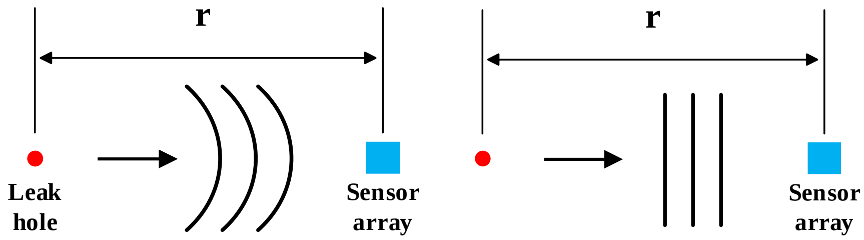

(a) Near-field model (b) Far-field model

Figure 2. Models of the beamforming localization method

In a leak localization system based on the beamforming technique a number of factors should be considered in the selection of the field model. For the continuous CO_2 leak signal from 100 kHz to 200 kHz, the acoustic wave speed ranges from 3000 m/s to 6000 m/s in a metallic flat-surface structure, thus the wavelength of the leak signal varies between 15 mm and 60 mm. In view of the size of the AE sensor and permissible installation area, the length of the linear sensor array is 0.5 m as an example, the separated region of the near-field model and the far-field model is thus about 8.3 m to 33.3m. This means that the near-field model is more appropriate for an apparatus which the length or width is no greater than 8.3 m, such as a laboratory-scale test rig.

The aim of this paper is to determine the location of the leak hole in a two-dimensional plane through the application of the beamforming technique. Suppose a linear AE sensor array consisting of *N* sensors is arranged in the near-field model, as shown in figure 3.

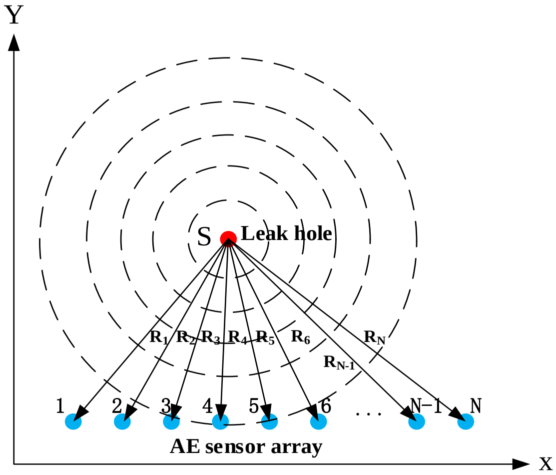

Figure 3. A linear AE sensor array in the near-field model

The coordinates of each sensor are known when the sensor array is arranged. With reference to figure 3, (X_s, Y_s) are the coordinates of the leak hole, (X_i, Y_i), i=1 … N, are the coordinates of sensor i, R_i is the distance between the leak hole and sensor i, and c is the speed of the acoustic waves. Taking sensor 1 as the reference sensor, so the time difference between sensor 1 and sensor i can be calculated as follows:

$$R_i = \sqrt{(X_s - X_i)^2 + (Y_s - Y_i)^2} \quad (3)$$

$$\tau_i = \frac{R_i - R_1}{c} \quad (4)$$

Suppose $s(t)$ is the signal of the reference sensor, $n(t)$ is the noise, and f is the central frequency of the signal, then

$$s(t) = ae^{j\omega t} = ae^{j2\pi ft} \quad (5)$$

where a is the amplitude of the signal. The signal received by sensor i, $x_i(t)$, can be expressed as:

$$x_i(t) = s(t)e^{-j2\pi f\tau_i} + n_i(t) \quad (6)$$

Therefore, signals received by the sensor array can be expressed by:

$$X(t) = A(X_s, Y_s)s(t) + N(t) \quad (7)$$

where $X(t) = [x_1(t), x_2(t), \dots, x_N(t)]^T$, $N(t) = [n_1(t), n_2(t), \dots, n_N(t)]^T$, and $A(X_s, Y_s) = [1, e^{-j2\pi f\tau_2}, \dots, e^{-j2\pi f\tau_N}]^T$.

In practice, the location of the leak hole is unknown and need to be identified. Assume any point P(X_0, Y_0) in the two-dimensional plane is the leak hole, then signals received by the sensor array can be expressed as:

$$Y(t) = W(X_0, Y_0)s(t) + N(t) \quad (8)$$

where the weighting vector $W(X_0, Y_0)$ is calculated from:

$$W(X_0, Y_0) = [1, e^{-j2\pi f\frac{R_{02} - R_{01}}{c}}, \dots, e^{-j2\pi f\frac{R_{0N} - R_{01}}{c}}]^T \quad (9)$$

Where

$$R_{0i} = \sqrt{(X_0 - X_i)^2 + (Y_0 - Y_i)^2} \quad (10)$$

Then, the output energy of the sensor array Q at the leak point P is given by:

$$Q = E\{X(t)Y^T(t)\} = E\{A(X_s, Y_s)s(t)s^T(t)W(X_0, Y_0)^T\} \quad (11)$$

Figure 4 shows the principle of the near-field beamforming technique: searching the largest output energy point or zone by scanning all the possible points in the field.

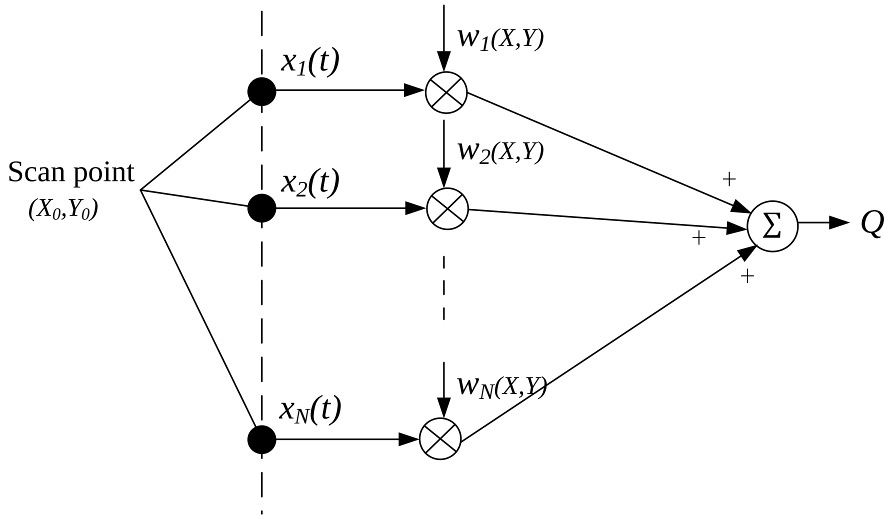

Figure 4. Schematic of the near-field beamforming

An energy distribution graph of the scanning field can be drawn by scanning all the points in the field and calculating the corresponding output energy of the sensor array. When the scanning point (X_0, Y_0) is just at the leak hole (X_s, Y_s), the two signals $X(t)$ and $Y(t)$ have the same phase, so the output energy of the sensor array reaches a maximum and hence a peak point in the energy distribution graph. In order to achieve accurate localization of continuous CO_2 leaks, a narrow-band signal filtering technique is deployed because acoustic waves have different speeds and modes with different frequencies. According to the definition of a narrow band signal, the frequency bandwidth of the signal and the central frequency must comply with the following relationship [20]:

$$B/f_0 < 1/10 \tag{12}$$

where B is the frequency bandwidth and f_0 the central frequency of the signal.

Figure 5 shows the logical steps in the proposed near-field beamforming localization method with a linear AE sensor array and the narrowband filtering technology.

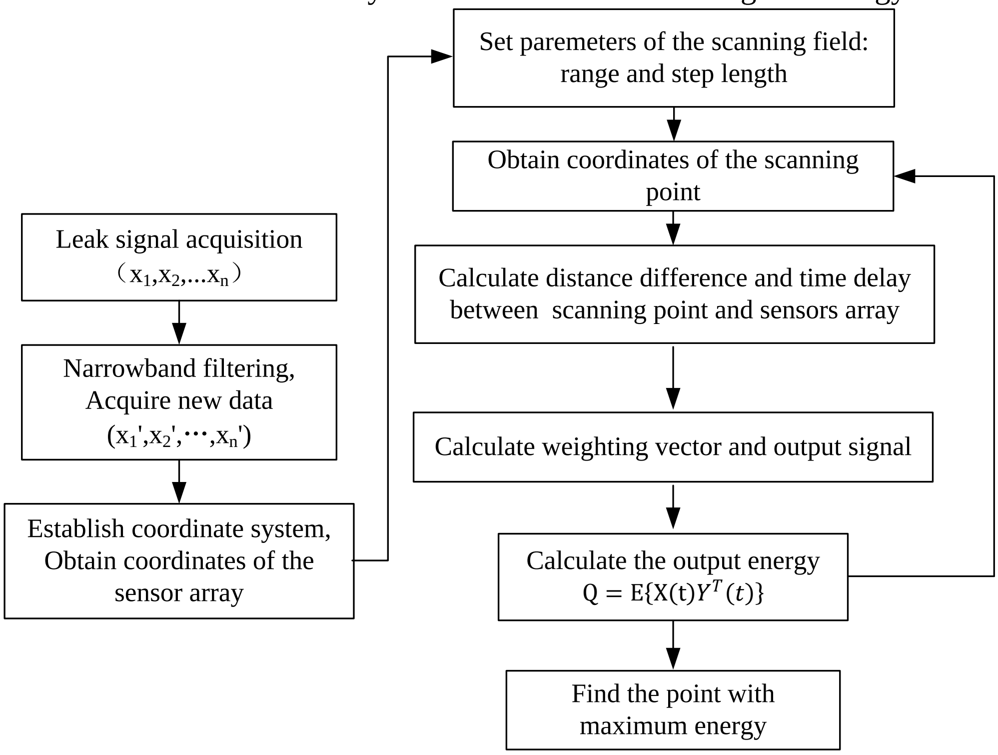

Figure 5. Logical steps in the near-field beamforming leak localization

3. Numerical Simulation

In order to optimize the sensor arrangement, the impact of various factors on the performance of the localization technique should be studied through computer simulation. The factors considered include the number of sensors, distance between the leak hole and sensor array and spacing between adjacent sensors.

Assume a leak hole is located in (50 cm, 50 cm) on a flat-surface structure, the linear sensor array is composed of six AE sensors and the coordinate of the first sensor is (20 cm, 20 cm). The distance between adjacent sensors is set to 10 cm. Scanning range is from 0 cm to 100 cm both in the x and y dimensions with an increment of 1 cm. The central frequency and amplitude of the simulated signal are 160 kHz and 1, respectively. The time domain waveforms of signal $s(t)$ is shown in figure 6.

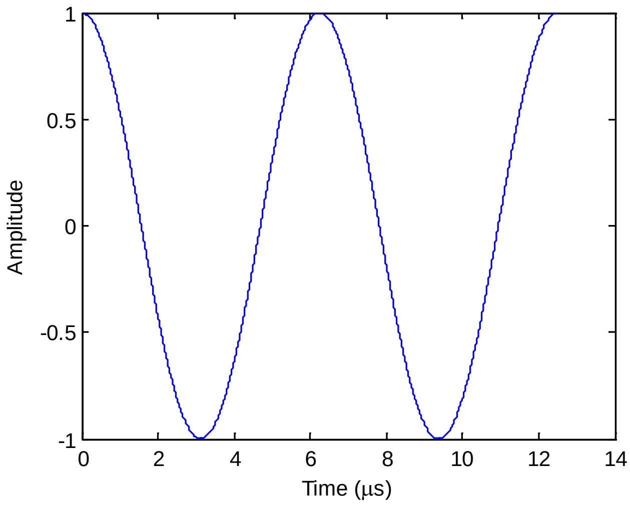

Figure 6. Time domain waveforms of signal $s(t)$

Figure 7 shows the energy distribution across the whole scanning area. The white square in the center indicates the high-energy gathering area. The white round dot within the white square marks the point with the maximum energy, the symbol ‘o’ indicates the location of the sensor array. The energy scale is normalized to the range between 0 and 1.

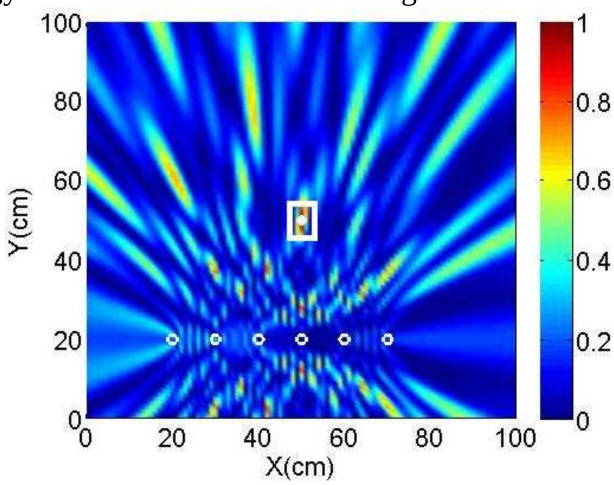

Figure 7. Energy distribution graph

It can be seen from figure 7 that there is a clear high-energy gathering area in the center of the flat-surface structure. The maximum energy point is located at (50 cm, 50 cm), which is the same as the hypothetical leak hole. This result indicates good localization performance using the proposed near-field beamforming technique.

3.1 Number of sensors

In order to investigate the influence of the number of sensors in the array on the localization performance of the technique, the number of sensors is set to 4, 6 and 8, respectively, and other parameters are the same as figure 7. Energy distribution graphs are shown in figure 8, (a) is the energy distribution graph with 4 sensors, (b) and (c) are the energy distribution graphs with 6 and 8 sensors, respectively.

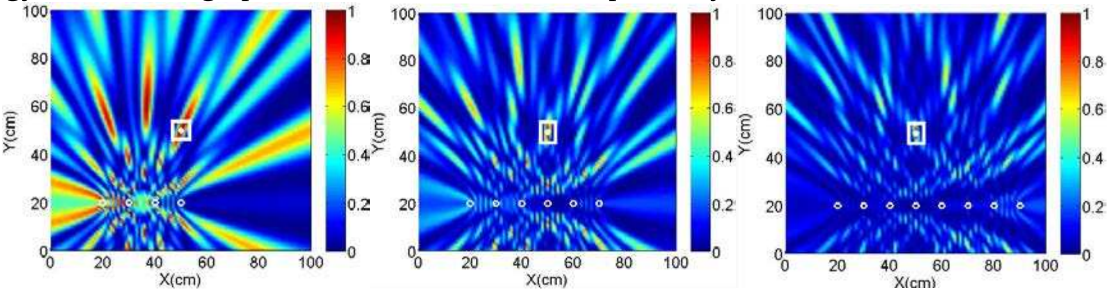

(a) n=4 (b) n=6 (c) n=8

Figure 8. Energy distribution for a different number of sensors in the array

Figure 8 shows that the localization performance becomes much better with the increase of the number of sensors in the array. In figure 8(a), although the highest energy gathering area (main lobe) and the point with the maximum energy are located near the leak hole, there are many other high-energy areas in the surrounding (side lobes). The presence of these side lobes may affect the localization result seriously and sometime even lead to a wrong localization result. In figures 8(b) and 8(c), the localization performance has improved significantly and there is only one obvious high energy gathering area which is just in the leak hole. It can be seen that the main lobe becomes narrower, the number and energy amplitude of side lobes turn less and smaller, respectively, with the increase of the number of sensors. This result suggests that the number of sensors should be large enough to maintain the localization resolution in the use of the near-field beamforming technique.

3.2 Distance between the leak hole and sensor array

In order to investigate the effect of the distance between the leak hole and sensor array on the localization performance, the coordinate on the Y axis of the sensor array is set to 10 cm, 20 cm and 40 cm, respectively, and other parameters are the same as figure 6. This means the sensor array is placed closer to the leak hole. Figure 9 shows the resulting energy distributions.

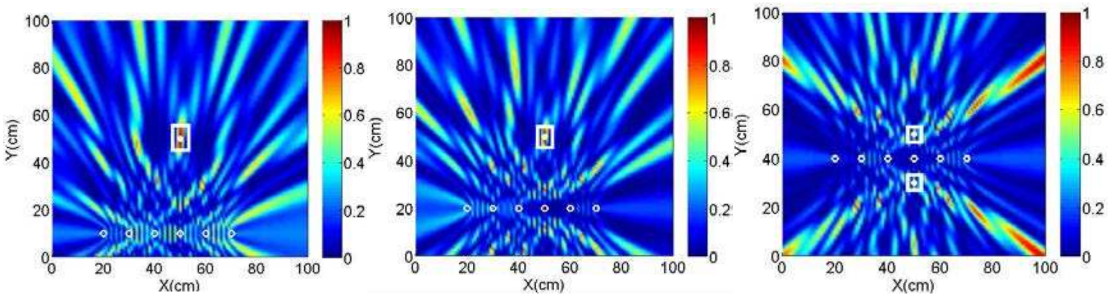

(a) y=10 cm (b) y=20 cm (c) y=40 cm

Figure 9. Energy distribution for different distance between the leak hole and sensor array

Both figure 9(a) and figure 9(b) show good localization performance, however, a pseudo leak hole emerges unexpectedly in figure 9(c). The reason for this phenomenon is that the energy distribution is symmetrical when the sensor array is very close to the leak hole, where the sensor array acts like a mirror. In addition, there are four high-energy side lobes in the corners of the scanning field, which will lead to the increase in the localization error.

3.3 Spacing between adjacent sensors

In order to investigate the effect of the spacing between adjacent sensors on the localization performance, the spacing between adjacent sensors is set to 5 cm, 10 cm and 15 cm, respectively, and other parameters are the same as figure 7. The resulting energy distributions are plotted in figure 10.

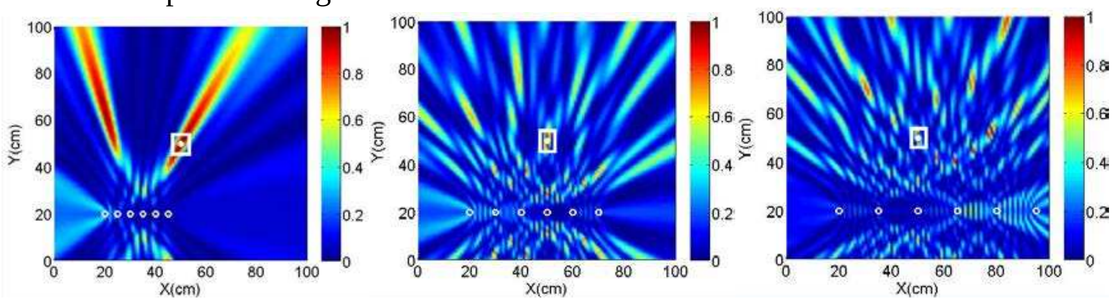

(a) s = 5 cm (b) s = 10 cm (c) s = 15 cm

Figure 10. Energy distribution for different sensor spacing

A comparison of the three graphs in figure 10 indicates that the localization performance deteriorates when the spacing between adjacent sensors is too short (Figure 10(a)). The existence of the high-energy side lobes will affect the determination of the point with the maximum energy and thus increased localization error. It is interesting to note that a far-field model instead of a near-field model should be considered when the spacing between adjacent sensors is small. On the other hand, when the spacing between adjacent sensors is exceedingly large, compared to the distance from the leak hole to the sensor array, the energy of the main lobe and side lobes becomes very similar, which may lead to large localization error (Figure 10(c)).

In summary, in order to increase the localization accuracy of the near-field beamforming technique, a sufficient number of sensors should be used to ensure the scanning resolution. Further, the distance between the leak hole and sensor array should not be too close. If there are two points with maximum energy in the energy distribution and symmetrically distributed about the sensor array in a row, either of these two points can be the leak hole and other methods should be deployed to identify which one is the leak hole such as by adding a sensor above or below the sensor array. Moreover, the spacing between adjacent sensors in the array should be comprehensively considered as per the size of the scanning field and the number of sensors available.

4. Experimental Evaluation

4.1 Experimental set-up

Experiments were carried out on a 316L stainless plate with dimensions of 100 cm × 100 cm × 0.2 cm. A simulated continuous leak of CO_2 was created at a pressure of 2 bar from a circular shaped hole with 2 mm diameter in the center of the plate. A linear array with six AE sensors was mounted on the plate using vacuum grease couplant. Leak signals were pre-amplified using AE amplifiers with a bandwidth of 10 kHz – 1 MHz at 40 dB amplification to reduce the influence of noises and interferences. A 6-channel holographic AE signal recorder (DS-8A) was used for waveform acquisition at a sampling rate of 3 MHz. The experimental set-up and sensor arrangement are shown in figure 11. The main technical specifications of the AE sensors are summarized in table 1.

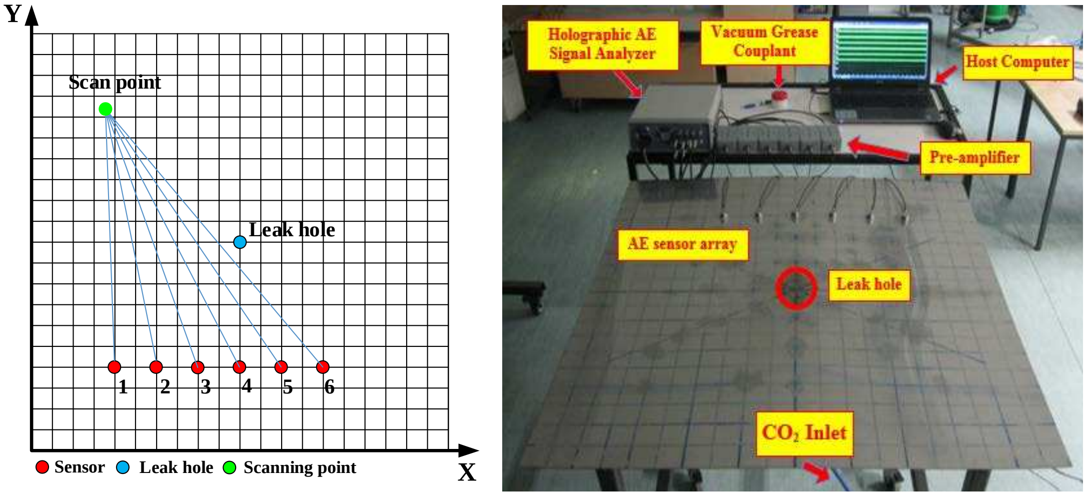

(a) Schematic of the set-up (b) Photo of the set-up

Figure 11. Experimental set-up and sensor arrangement

Table 1 Technical specifications of the AE sensor

Diameter	18.8 mm
Height	15 mm
Interface type	M5-KY
Operating frequency range	50-400 kHz
Operating temperature	-20~200 ℃

4.2 Results and discussion

4.2.1 Signal characteristics

The signals from the sensor array are very similar to each other due to the fact that they are mounted close to each other and used to detect the same leak source. Take the signal from sensor 1 as an example, the time domain waveform and corresponding frequency spectrum are plotted in figures 12 and 13, respectively.

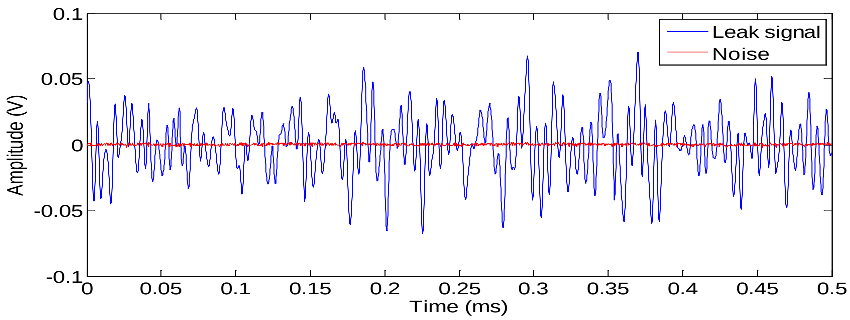

Figure 12. Time domain waveforms of the leak signal and noise

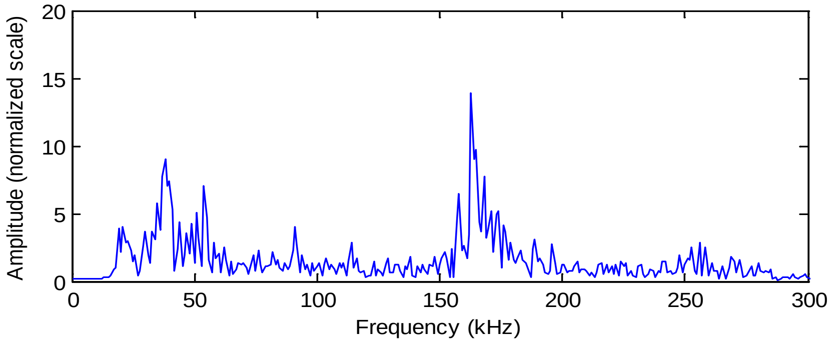

Figure 13. Frequency spectrum of the leak signal

It can be seen from figures 12 and 13 that the leak signal is continuous in the time domain and has a wide spectral range from 20 kHz to 300 kHz. The leak signal contains frequency components in two main regions, one in the high frequency band (150 kHz - 180 kHz), and the other in the low frequency band (30 kHz - 50 kHz). Since the high frequency region is not adversely affected by the ambient noise, the signal in this region is utilized for the leak localization in this study. Figure 12 also indicates that the noise of the detection system is very low with an amplitude of no greater than 5mV.

4.2.2 Leak localization results and error analysis

For the linear AE sensor array in figure 11(a), the overall span of the linear sensor array is 50 cm. The spacing between adjacent sensors is 10 cm. The leak hole is located at the center of the plate (50 cm, 50cm).

The leak signal contains a wide range of frequencies whilst the acoustic waves have different speeds and modes with different frequencies, which all increase the difficulties in locating the leak hole. In order to achieve more accurate localization of a continuous CO_2 leak, an FIR (finite impulse response) narrow-band digital filter is deployed in recognition of its advantages such as high precision, high reliability and flexibility in configuring the filter characteristics over analogue and other digital filters. In addition, the FIR filter has a linear phase response, which means the phase information of the leak signal containing different frequency components is maintained after the filtering. The narrow-band FIR filter was designed using MATLAB Filter Design and Analysis Tool. The frequency band of the filter is [155 kHz, 165 kHz], thus the central frequency is 160 kHz and frequency band is 10 kHz, which comply with the relationship of a narrow band signal. The speed of the acoustic wave near the frequency of 160 kHz is 4000 m/s, which was measured by combining the Nielsen-Hsu Pencil Lead Break Test [21] and the narrow-band signal filtering technique.

Figure 14 shows a typical localization result. The leak hole is found to be located at (50 cm, 55 cm) by searching the maximum output energy across the whole plate, as the white round dot shown in figure 14.

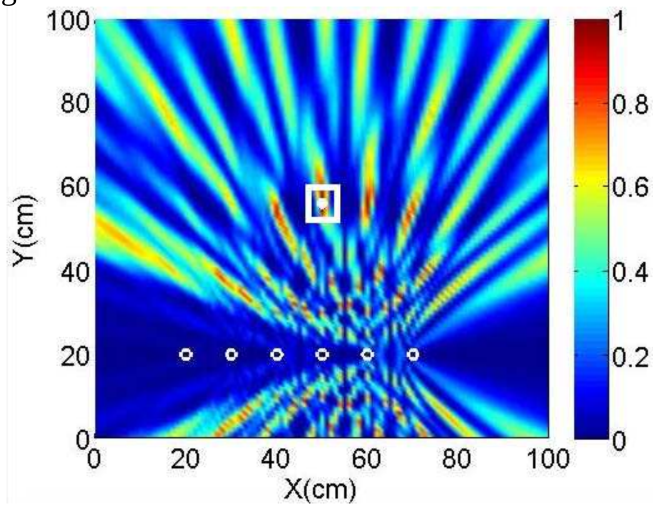

Figure 14. Leak localization result

In order to assess the accuracy and stability of the proposed method, experiments were repeated for 10 times. Results are plotted in figure 15.

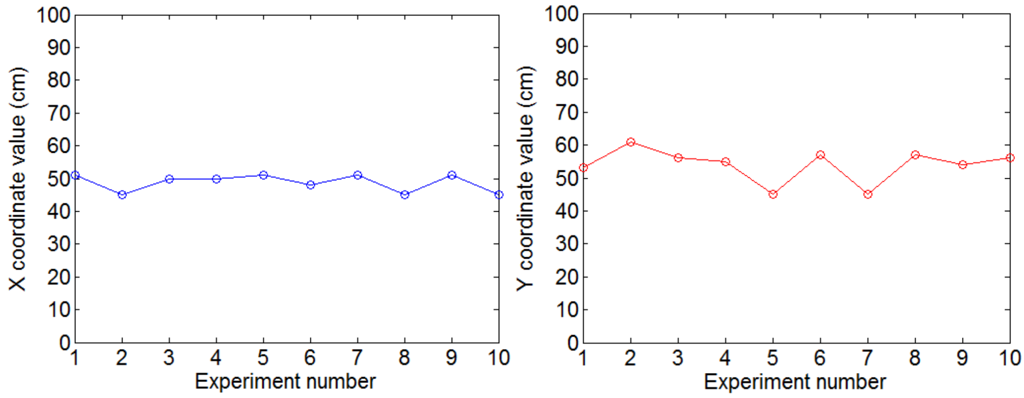

(a) X coordinate (b) Y coordinate

Figure 15. Localization results of 10 repeated experiments

It can be seen from figure 15 that all the measured coordinates are around 50 cm. Given the coordinates of the actual leak hole (50 cm, 50 cm), this result indicates that the localization method based on the near-field beamforming principle is capable of locating the position of a continuous CO_2 leak effectively. The final measured coordinates of the leak hole by averaging the repeated experimental results are (48.7 cm， 53.9 cm) with standard deviations of (2.7 cm, 5.2 cm). The reason for the smaller error in X coordinate is that the sensor array is arranged in a straight line in parallel with the X axis, as a result, the measured X coordinate is less uncertain than the Y coordinate. This result suggests that the linear sensor array has a higher accuracy in the axis in parallel with the sensor array. The absolute error in the dimensional measurement on the flat surface (i.e. the absolute distance between the measured location and expected location of the leak hole) is 4.1 cm, which is equivalent to a full-scale error of 4.1% (The full-scale error is defined as the absolute error normalized to the full length of the square plate).

In this paper, the localization results were calculated off-line using a personal computer (Intel Celeron(TM) i5-3230M @ 2.60GHz, RAM 4GB, 64bits Windows 7) and the computation time including image display was 1.35s. It is worth noting that the computation time depends also on the scanning condition. The scanning range in this study is from 0 cm to 100 cm both in the x and y dimensions with an increment of 1 cm. In practical leak localization applications, the computation time can be shortened deploying a faster computer or embedded system and optimizing the scanning range and the scanning step.

5. Conclusions

A novel localization method based on a linear acoustic emission sensor array and a near-field beamforming technique has been proposed to locate the continuous CO_2 leaks from an isotropic flat-surface structure. The impacts of various factors on the performance of the localization method have been simulated and compared. These include the number of sensors, distance between the leak hole and sensor array, and spacing between adjacent sensors in the array. The simulation results have suggested that a sufficient number of sensors should be used to ensure the scanning resolution and that the distance between the leak hole and the sensor array should not be excessively close. If there are two points with maximum energy in the energy distribution and symmetrically distributed about the sensor array in a row, anyone of these two points can be the leak hole. The spacing between adjacent sensors in the array should be considered based on the size of the scanning field and the number of sensors. Experiments were carried out on a laboratory-scale test rig and leak signals were collected by a linear high-frequency sensor array. Time-frequency analysis results have indicated that the leak signal contains frequency components in two main regions, one in the high frequency band (150 kHz - 180 kHz), the other in the low-frequency band (30 kHz - 50 kHz). A narrow band and high frequency signal with the central frequency 160 kHz and frequency band 10 kHz has been obtained through the use of a narrow band FIR filter. The narrow-band, high-frequency signal has been employed to identify the location of the leak hole using the near-field beamforming technique. The results have demonstrated that the full-scale error in the leak localization measurement is 4.1% on a 100 cm × 100 cm plate.

Acknowledgement

The authors wish to acknowledge the Chinese Ministry of Science and Technology (MOST) and the Chinese Ministry of Education for providing financial support for this research as part of the 111 Talent Introduction Projects (B13009) at North China Electric Power University. This work was also supported by the Fundamental Research Funds for the Central Universities (No. 2014XS40, 2015XS64). Xiwang Cui would like to thank the China Scholarship Council for offering an academic exchange grant for his visit to the University of Kent.

Reference

[1] J. Gibbins, H. Chalmers. Carbon capture and storage. Energy Policy, 2008, 36(12): 4317-4322.

[2] P. S. Murvay, I. Silea. A survey on gas leak detection and localization techniques. Journal of Loss Prevention in the Process Industries, 2012, 25(6): 966-973.

[3] T. Iseki, H. Tai, K. Kimura. A portable remote methane sensor using a tunable diode laser. Measurement Science and Technology, 2000, 11(6): 594.

[4] K. Adefila, Y. Yan. A compendium of CO_2 leakage detection and monitoring techniques in carbon capture and storage (CCS) pipelines. EUROCON, 2013 IEEE, Zagreb: 1328-1335.

[5] A. Mostafapour, S. Davoudi. Analysis of leakage in high pressure pipe using acoustic emission method. Applied Acoustics, 2013, 74(3): 335-342.

[6] W. Tao, W. Dongying, P. Yu P, et al. Gas leak localization and detection method based on a multi-point ultrasonic sensor array with TDOA algorithm. Measurement Science and Technology, 2015, 26(9): 095002.

[7] T. Kundu, H. Nakatani, N. Takeda. Acoustic source localization in anisotropic plates. Ultrasonics, 2012, 52(6): 740-746.

[8] P. Liao, M. Cai, Y. Shi, et al. Compressed air leak detection based on time delay estimation using a portable multi-sensor ultrasonic detector. Measurement Science and Technology, 2013, 24(5): 055102.

[9] F. Ciampa and M. Meo. Acoustic emission source localization and velocity determination of the fundamental mode A0 using wavelet analysis and a Newton-based optimization technique. Smart Materials and Structures, 2010, 19(4): 045027.

[10] H. Nakatani, T. Kundu, N. Takeda. Improving accuracy of acoustic source localization in anisotropic plates. Ultrasonics, 2014, 54(7): 1776-1788.

[11] S. Davoodi, A. Mostafapour. Gas leak locating in steel pipe using wavelet transform and cross-correlation method. The International Journal of Advanced Manufacturing Technology, 2014, 70(5-8): 1125-1135.

[12] X. Cui, Y. Yan, Y. Ma, et al. Localization of CO_2 leakage from transportation pipelines through low frequency acoustic emission detection. Sensors and Actuators A: Physical, 2016, 237: 107-118.

[13] S. D. Holland, R. Roberts, D. E. Chimenti, et al. An ultrasonic array sensor for spacecraft leak direction finding. Ultrasonics, 2006, 45(1): 121-126.

[14] S. D. Holland, R. Roberts, D. E. Chimenti, et al. Two-sensor ultrasonic spacecraft leak detection using structure-borne noise. Acoustics Research Letters Online, 2005, 6(2): 63-68.
[15] S. D. Holland, R. Roberts, D. E. Chimenti, et al. Leak detection in spacecraft using structure-borne noise with distributed sensors. Applied Physics Letters, 2005, 86(17): 174105.
[16] S. A. Jafar, A. Goldsmith. Transmitter optimization and optimality of beamforming for multiple antenna systems. IEEE Transactions on Wireless Communications, 2004, 3(4): 1165-1175.
[17] G. C. McLaskey, S. D. Glaser, C. U. Grosse. Beamforming array techniques for acoustic emission monitoring of large concrete structures. Journal of Sound and Vibration, 2010, 329(12): 2384-2394.
[18] T. He, D. Xiao, Q. Pan, et al. Analysis on accuracy improvement of rotor–stator rubbing localization based on acoustic emission beamforming method. Ultrasonics, 2014, 54(1): 318-329.
[19] X. Bian, Y. Zhang, Y. Li, et al. A new method of using sensor arrays for gas leakage location based on correlation of the time-space domain of continuous ultrasound. Sensors, 2015, 15(4): 8266-8283.
[20] R. J. Mailloux. Phased array antenna handbook. Boston, MA: Artech House, 1994.
[21] M. G. Sause. Investigation of pencil-lead breaks as acoustic emission sources. Journal of Acoustic Emission, 2011, 29: 184-196